

Research paper

Cochlear developmental defect and background-dependent hearing thresholds in the Jackson circler (*jc*) mutant mouse

Alfredo Calderon ^a, Adam Derr ^a, Barden B. Stagner ^b, Kenneth R. Johnson ^c,
Glen Martin ^b, Konrad Noben-Trauth ^{a,*}

^a Section on Neurogenetics, Laboratory of Molecular Biology, National Institute on Deafness and Other Communication Disorders, National Institutes of Health, 5 Research Court, Rockville, MD 20850, USA

^b Jerry Pettis Memorial Veterans Medical Center, Loma Linda, CA 92357, USA

^c The Jackson Laboratory, Bar Harbor, ME 04609, USA

Received 22 May 2006; received in revised form 19 July 2006; accepted 20 July 2006

Available online 7 September 2006

Abstract

Jackson circler (*jc*) is a spontaneous, recessive mouse mutation that results in circling behavior and an impaired acoustic startle response. In this study, we refined the phenotypic and genetic parameters of the original *jc* mutation and characterized a new mutant allele, *jc^{2J}*. In open-field behavior tests, homozygous *jc* mutants exhibited abnormal circling and ambulatory behavior that was indistinguishable from that of phenotypically similar mutants with defects in the vestibule of the inner ear. The *jc/jc* and *jc^{2J}/jc^{2J}* mice had stable elevated auditory-evoked brainstem response (ABR) thresholds at the 16 kHz stimulus of 88 ± 9 dB sound pressure levels (SPL) and 43 ± 11 dB SPL, respectively. Peak latencies and peak time intervals were normal in *jc* mutants. The *jc* mice showed no measurable distortion-product otoacoustic emissions (DPOAEs) above the system noise floor. In the mutant cochlea, the apical turn failed to form due to the developmental growth arrest of the cochlear duct at the level of the first turn at gestational day 13.5. In a large intraspecific intercross, *jc* localized to a 0.2cM interval at position 25cM on chromosome 10, which is homologous to the human 6q21 region. On CZECHII/Ei and CAST/Ei backgrounds *jc/jc* mutant hearing thresholds at the 16 kHz stimulus were significantly lower than those observed on the C57BL/6J background, with means of 62 ± 22 dB SPL and 55 ± 18 dB SPL, respectively. Genome-wide linkage scans of backcross, intercross, and congenic progeny revealed a complex pattern of genetic and stochastic effects.

© 2006 Elsevier B.V. All rights reserved.

Keywords: Jackson circler; Hearing loss; Vestibular deficits; Cochlea malformation; Genetic background

1. Introduction

The recessive Jackson circler (*jc*) mutation arose spontaneously in the C57BL/6 mouse strain at The Jackson Laboratory in 1963 (Southard, 1970). Homozygous mutants were recognized by their erratic circling behavior and the absence of a startle reflex at three to five weeks of age.

Abbreviations: ABR, auditory brainstem response analysis; DPOAE, distortion-product otoacoustic emission; QTL, quantitative trait locus

* Corresponding author. Tel.: +1 301 402 4223; fax: +1 301 435 4040.

E-mail address: nobentk@nidcd.nih.gov (K. Noben-Trauth).

The mutation was initially linked to the *Steel* locus on linkage group IV (Southard, 1970) and was placed at position 32cM on chromosome 10 near marker *D10Mit30* of the Mouse Genome Informatics consensus map (MGD, 2005). Allelism tests with the closely linked deafness mutations waltzer (*Cdh23^v*) and Ames waltzer (*Pcdh25^{av}*) proved negative (MGD, 2005). Recent studies showed that mutations underlying a deafness/waltzing phenotype occur preferentially in genes encoding proteins that are targeted to stereocilia where they regulate organization, structure, growth and function of the hair bundle (Hasson et al., 1995; Mburu et al., 2003; Rzadzinska et al., 2004; Siemens

et al., 2002; Steel and Kros, 2001; Zheng et al., 2000). In these mutants the stereocilia defects become apparent in the postnatal period coinciding with the functional maturation of the hair cells. Mutations affecting the formation and patterning of the cochlea however manifest during late embryogenesis, and also affect other developmental pathways most notably the neural tube (Cordes and Barsh, 1994; Curtin et al., 2003; Montcouquiol et al., 2003; Phippard et al., 1999; Quint and Steel, 2003). The isolated and pronounced circling phenotype of Jackson circler mice suggested that the *jc* gene is critical for hair cells during post-natal growth.

Phenotypic characteristics of a trait are often influenced by allelic variants present in the genetic background (Nadeau, 2001). Hearing screens in mouse strains, conducted by measuring auditory-brainstem response thresholds and distortion-product otoacoustic emissions, have revealed substantial variation within and among strains with respect to onset and progression of hearing loss (Jimenez et al., 1999; Zheng et al., 1999). Quantitative trait loci underlying this phenotypic variance could be localized in some inbred strains (for review see (Johnson et al., 2006)). Intra-strain variation, such as that seen in C57BL/6J more than one year of age and in CBA/CaJ mice around two years of age is thought to result from the breakdown of homeostatic mechanisms and environmental effects (Hequembourg and Liberman, 2001; Keithley et al., 2004). Epistatic interactions and genetic modifiers altering the disease outcome of pathological hearing loss alleles introduce additional variation (Ikeda et al., 1999; Nadeau, 2003; Noben-Trauth et al., 1997). Methodical analyses of the background variation identified new alleles linked with hearing loss (Johnson et al., 2006) and it is thought that such hypomorphic alleles and a combination thereof contribute to non-Mendelian forms of hearing impairment.

In this work, we characterize different aspects of the inner ear phenotype of the Jackson circler mutant, describe a new allele, present a high-resolution genetic map, and report on the effect of the genetic background on the hearing threshold distribution.

2. Materials and methods

2.1. Mice

All strains used in this study were obtained from The Jackson Laboratory (Bar Harbor, ME, USA). The strain carrying the original *jc* mutation is designated C57BL/6J-*jc*/J (STOCK #563). The *jc*^{2J} mutation arose spontaneously in the B6.129S6-*Il6*^{tm1Kopf} colony (STOCK #2650) and was given the official strain name B6(129S6)-*jc*^{2J}/J (STOCK #5292). Selective breeding against segregation of the *Il6*^{tm1Kopf} allele (located on chromosome 11) eliminated the targeted mutation from the *jc*^{2J} stock. Homozygous *jc*^{2J} mutants show the typical circling behavior and are able to swim.

The wild-derived CAST/Ei and CZECHII/Ei strains were used in the mapping crosses to obtain a high degree of heterogeneity at marker loci and to introduce phenotypic diversity in the cross. To map the *jc* mutation an intercross scheme was chosen to obtain the optimal number of meioses per offspring. To map genetic modifiers alternative crosses and schemes were used to test for experimental reproducibility and robustness of statistical significance levels. C57BL/6J-*jc*/*jc* males and females were crossed with CZECHII/Ei and offspring were intercrossed to produce the B6/CZECH-F2 population. To generate B6/CAST-F2 progeny, C57BL/6J-*jc*/*jc* males were crossed to CAST/Ei females and the resulting F1 hybrids were intercrossed. To obtain B6/CZECH-N2 offspring, C57BL/6J-*jc*/*jc* males were crossed with CZECHII/Ei females, and female F1 hybrid females were backcrossed to C57BL/6J-*jc*/*jc* males. For serial backcrossing, B6/CZECH-*jc*/*jc* males were crossed to C57BL/6J+/+ females. All animal studies followed the guidelines of the National Institutes of Health and were approved by institutional review boards.

2.2. Open-field behavior

Movement and activity behavior were measured using an Opto-Varimex 3 Activity Monitor from Columbus Instruments (Columbus, OH, USA). Briefly, each mouse was placed in a 7.5 in. × 8 in. × 12 in. (W × H × L) cage, situated in a 17 in. × 17 in. × 8 in. open-field apparatus equipped with one row each of horizontal and vertical sensors, with each row consisting of 15 infrared beams, such that the horizontal and vertical beams were perpendicular to one another. The beams were one inch apart and 3 mm in diameter. Movements were tracked for 60 min and each test was repeated at least three times. Data were collected and analyzed using the Auto-Track v3.4 from Columbus Instruments. Ambulatory time (AT) was the time (measured in seconds, s) the animal exceeded the minimal field. The *x*- and *y*-beam defined minimal field was 5.8 cm². Clockwise (CR) and counter-clockwise (CCR) rotations were defined as four consecutive right-handed or left-handed changes in direction, respectively. Two common laboratory strains (C57BL/6J and C3HeB/FeJ) and three wild-derived strains (CAST/Ei, CZECHII/Ei and MOLF/Ei) were included in the study to serve as genetic background controls for the various mutant alleles and to ascertain the variability among inbred strains.

2.3. Auditory-evoked brain stem response (ABR) analyses

ABR testing was performed as previously described (Zheng et al., 1999). All mice were presented with click, 8-, 16-, and 32-kHz stimuli at intensities varying between 10 and 100 dB SPL. Each stimulus was presented 350 times at a rate of 19 s⁻¹ using a Blackman filter. Filter settings used 100 Hz for high-pass and 3 kHz for low-pass. Animals were anesthetized using tribromethanol. ABR measurements

were taken for offspring of C57BL/6J-*+jlc* × C57BL/6J-*jcljc* matings. Unless otherwise indicated, ABR thresholds were given as the mean ± one standard deviation. The mean ages of mice at the time of weaning were 87 ± 5 days for the (CAST/Ei × C57BL/6J-*jcljc*) F1 × F1 intercross progeny, and 47 ± 7 days for the (CZECHII/Ei × C57BL/6J-*jcljc*) F1 × F1 intercross progeny, and 49 ± 8 days for the (CZECHII/Ei × C57BL/6J-*jcljc*) × C57BL/6J-*jcljc* backcross progeny.

2.4. Distortion-product otoacoustic emission measurements

Distortion-product otoacoustic emissions (DPOAEs) were measured in five C57BL/6J-*jcljc* and five C57BL/6J-*+jlc* mice at 3 months of age. The $2f_1 - f_2$ DPOAE measurements were performed as previously described for mice (Jimenez et al., 1999; Vazquez et al., 2001). Briefly, DPOAEs were produced by the simultaneous presentation of two pure tones at the f_1 and f_2 primary frequencies (f_2/f_1 ratio = 1.25) and levels (L_1 , L_2) specified below. The primary tones were generated by a dual-channel synthesizer (model 3326A, Hewlett-Packard, Palo Alto CA) and attenuated under the control of a personal computer system using customized software. The f_1 and f_2 primaries were presented over two separate ear speakers (Realistic® Dual Radial Horn Tweeters, Tandy Corp, Dallas TX) and delivered through a commercially available acoustic probe incorporating a calibrated microphone assembly (ER-10B+, Etymotic Research Elk Village, IL) that was inserted snugly into the outer ear canal. The two primary tones were allowed to mix acoustically in the ear canal to avoid artifactual distortion.

Ear-canal sound pressure was sampled and averaged using two methods. For f_2 frequencies from 6.3 to 22.5 kHz, sampling and averaging were performed by a digital signal processor (DSP) in the microcomputer. DPOAE levels were measured automatically over the 92-ms duration of the primary tones from the amplitude spectrum resulting from a 4096-point (bandwidth = 10.8 Hz) fast Fourier transform (FFT) of four synchronously averaged samples. To determine the corresponding noise floors (NFs), the levels for the ear-canal sound pressure for five FFT frequency bins above and below the DPOAE-frequency bin (i.e., ±54 Hz) were averaged.

For f_2 frequencies from 21.5 to 54.2 kHz, a computer-controlled dynamic-signal analyzer (3561A, Hewlett-Packard, Palo Alto CA) was used. Within this higher-frequency test range the DPOAE levels were based upon the results of four spectral averages of the ear-canal signal. For this method NFs were estimated by averaging the levels of the ear-canal sound pressure for the two FFT frequency bins below the DPOAE frequency (i.e., for 3.75 Hz below the DPOAE). Using either the DSP- or signal-analyzer systems, no artifactual DPOAEs were ever measured in a hard-walled cavity that approximated the size of the mouse outer ear canal. DPOAEs were measured as DP-grams, i.e., DPOAE levels as a function of f_2 frequency. Three pri-

mary-tone levels were applied consisting of either $L_1 = L_2 = 55$, 65 or 75 dB SPL. These levels were selected because they have been shown to be effective in screening for cochlear defects in mice (Jimenez et al., 1999; Jimenez et al., 2001). All mice were tested while anesthetized with 1.5% concentration of isoflurane administered via a standard veterinarian inhalation anesthesia machine.

2.5. Paint fillings

The bony labyrinth of the inner ear at E13.5 and E15.5 (day of gestation, E) was paint-injected following the protocol described by Martin and Swanson (1993). Briefly, the heads were fixed in Bodian fixative (5% glacial acetic acid; 1.85% formaldehyde; 75% ethanol) for 12 h, dehydrated in a graded series of ethanol (75%; 95%; 100%), and cleared in methyl-salicylate (EM Science). The heads were bi-dissected, temporal brain tissue was removed and white latex paint (0.025% in methyl-salicylate) was injected into one of the ampulla. Pictures were taken on a Zeiss dissecting microscope using a DXM1200 digital camera (Nikon). Embryos were obtained from C57BL/6J-*+jlc* × C57BL/6J-*jcljc* and C57BL/6J-*jcljc* × C57BL/6J-*jcljc* matings. The time at which a maternal plug was observed was set as E0.5.

2.6. Crosses and genetic mapping

Reciprocal matings between C57BL/6J-*jcljc* and wild-derived inbred CZECHII/Ei mice (*Mus musculus musculus*) produced the B6/CZECH-*+jlc* F1 generation, which were intercrossed to generate 990 F2 offspring. F2 mice were phenotypically classified based upon their vestibular phenotype and their hearing thresholds. Non-informative recombinants were crossed to C57BL/6J-*+jlc* heterozygotes and offspring with informative genotypes were tested for hearing function by ABR analysis. *D10Mit* markers were obtained from Research Genetics (Invitrogen, Carlsbad, CA). *D10Ntra* (simple-sequence-length and single-nucleotide) polymorphic markers were developed in our laboratory. Primer sequences are available upon request. Genetic distances were computed using MapManager QTX software (Manly et al., 2001). The *jc* physical interval was analyzed using the Human Genome Browser at www.genome.cse.ucsc.edu (assembly May 2005). Chromosomal locations were obtained from the Mouse Genome Database at www.informatics.jax.org (Eppig et al., 2005).

2.7. Genotyping

Genomic DNA was extracted from tail clips using DNeasy™ (Qiagen, Valencia, CA). For amplification 20–50 ng of extracted DNA served as the template in a 10 µl reaction containing 0.2 µM each primer, 200 µM dNTP, 10 mM Tris-HCl, pH 8.3, 50 mM KCl, 1.5 mM MgCl₂, and 0.25 U AmpliTaq™ DNA polymerase (Applied Biosystems). The reactions were incubated at 95 °C for 1 min,

then cycled 50 times through 95 °C for 45 s, 55 °C for 1 min, 72 °C for 1 min, followed by a final extension at 72 °C for 10 min and cooled to 4 °C for 2 min. For capillary electrophoresis, 1 µl of amplified product was diluted 1:10 in formamide containing 0.1 µl GenScan™ 500 ROX™ size standard, separated on a 3730 DNA Analyzer (Applied Biosystems), and analyzed using GenMapper software v3.1 (Applied Biosystems). For agarose gel electrophoresis, PCR product was loaded on 4% Metaphor 1% NuSieve 3:1, separated and visualized with ethidium bromide staining.

2.8. Genome-wide linkage scan

Microsatellite markers that are polymorphic between C57BL/6J, and CAST/Ei mice were selected from the Center for Inherited Disease Research website (www.cidr.jhmi.edu/mouse/mouse_strp.html) (Witmer et al., 2003) and purchased from Applied Biosystems, Invitrogen or IDT. For the genome-wide scan on the B6/CZECH-*jc/jc* N2 population, 42 *jc/jc* progeny were genotyped at 137 marker loci. For the analyses of the B6/CAST-*jc/jc* F2 cross, a selective genotyping protocol was used. Twenty progeny from each tail of the hearing threshold distribution (40 F2 *jc/jc* homozygotes total), containing most of the genotypic information, were typed at 127 markers. For the scan on the B6/CZECH-*jc/jc* F2 cross, 45 *jc/jc* progeny were typed at 143 markers. The linear regression method of MapManager QTXb20 was used to analyze association of genotype data with trait values (Manly et al., 2001). Empirical thresholds to estimate genome-wide significance of likelihood-ratio-statistic (LRS) scores were computed by performing 1000 permutations (Churchill and Doerge, 1994). Genome-wide *p* values of 0.63 and 0.05 were taken as the suggestive and significant linkage levels, respectively (Lander and Kruglyak, 1995). Pair-wise marker regression analyses were performed at $p = 10^{-5}$ and the significance level for the interaction was computed by permutation testing. LRS scores were converted to LOD scores by dividing the LRS value by the factor $2\ln(10)$.

2.9. Statistical analyses

Descriptive statistics, analyses of variance (ANOVAs), Dunn's correction for multiple testing, and normality tests were performed using GraphPad Prism 4.0b software (San Diego, CA).

3. Results

3.1. Hyperactivity and circling behavior

To assess the vestibular deficits in Jackson circler mutants, we measured movement behavior in an open-field test system. During a 60-min test period, homozygotes spent significantly more time in ambulation than their heterozygous littermates ($p < 0.0001$; *t*-test). Specifically, *jc/jc*

mice ($n = 22$), six weeks of age and older, spent an average (\pm one standard deviation) of 1480 ± 540 seconds per hour (s/h) in non-stereotypic behavior compared to 576 ± 238 s/h of littermate controls ($n = 7$) (Fig. 1A; Table 1). Mice of the C57BL/6J and C3HeB/FeJ strains spent an average of 676 ± 309 s/h and 490 ± 173 s/h in ambulation, which was not different from the behavior of *+/jc* heterozygotes ($p > 0.05$, Dunnett's multiple comparisons test). Hyperactive behavior of *jc/jc* mutants was also significantly different from activities of the wild-derived CZECHII/Ei and CAST/Ei strains, which spent an average of 325 ± 119 s/h and 826 ± 315 s/h in ambulation, respectively ($p < 0.01$, Dunnett's multiple comparisons test).

As a general observation, the behavioral phenotype became apparent around weaning age, but full expression varied among individual mutants. The mean ambulation time in three-week old mutants was 684 s/h and had increased to 1321 s/h at six weeks of age (Fig. 1B, Table 1). Due to the wide scatter of data points there was no significant difference between the means of different age groups ($p > 0.05$, ANOVA). Ambulation behavior of *jc/jc* mice was compared with that of the phenotypically similar deaf waltzing mutants *Cdh23*^{v6J/v6J}, *Cdh23*^{v2J/v2J}, *Pcdh15*^{nmf19/nmf19}, *Esprn*^{je/je}, *Myo6*^{sv/sv}, *Myo15A*^{sh2/sh2}, and *Mcoln3*^{+Iva}. While there were clear differences between the mutants and the respective heterozygous or wildtype control group, the means of the mutant strains, including *jc*, were not significantly different from one another ($p > 0.05$; ANOVA) (Table 1).

A significant portion of the ambulatory behavior seemed to be correlated with extreme circling movements. Homozygous *jc/jc* mice ($n = 22$) performed 397 ± 464 clockwise (CRs) and 478 ± 675 counter-clockwise (CCRs) rotations per hour compared to 50 ± 48 CR and 45 ± 41 CRR in heterozygotes ($n = 7$). There was no significant difference in the direction of the circling motion among individual mutant mice ($p > 0.05$) (Fig. 1C). The combined CRs and CCRs ranged from 0 to 6255 rotations per hour. Ambulation and circling behavior showed a significant correlation ($p < 0.0001$) with a mean coefficient of determination (r^2 , Pearson) of 0.45 with upper and lower 95% confidence intervals of 0.17 and 0.73, respectively ($n = 5$) (Fig. 1D). Similar to the ambulation phenotype, there was no significant difference in circling behavior between *jc/jc* and other deaf waltzing mutants (Table 1). Finally, *jc* mutants covered a distance of 409 ± 125 m (maximum = 806 m) during a one-hour test, which deviated significantly from heterozygous littermates and normal inbred strains (Fig. 1E).

3.2. Auditory brain stem responses in *jc* and *jc*^{2J} mice

ABR measurements revealed that homozygous *jc* mice had measurable responses to click and pure tone stimuli, although at high sound pressure levels only. Two-week old *jc/jc* mutants ($n = 12$) had a mean hearing threshold of 83 ± 11 dB SPL to the click stimulus; individual thresholds ranged from 65 dB SPL to 100 dB SPL (Table 2). The

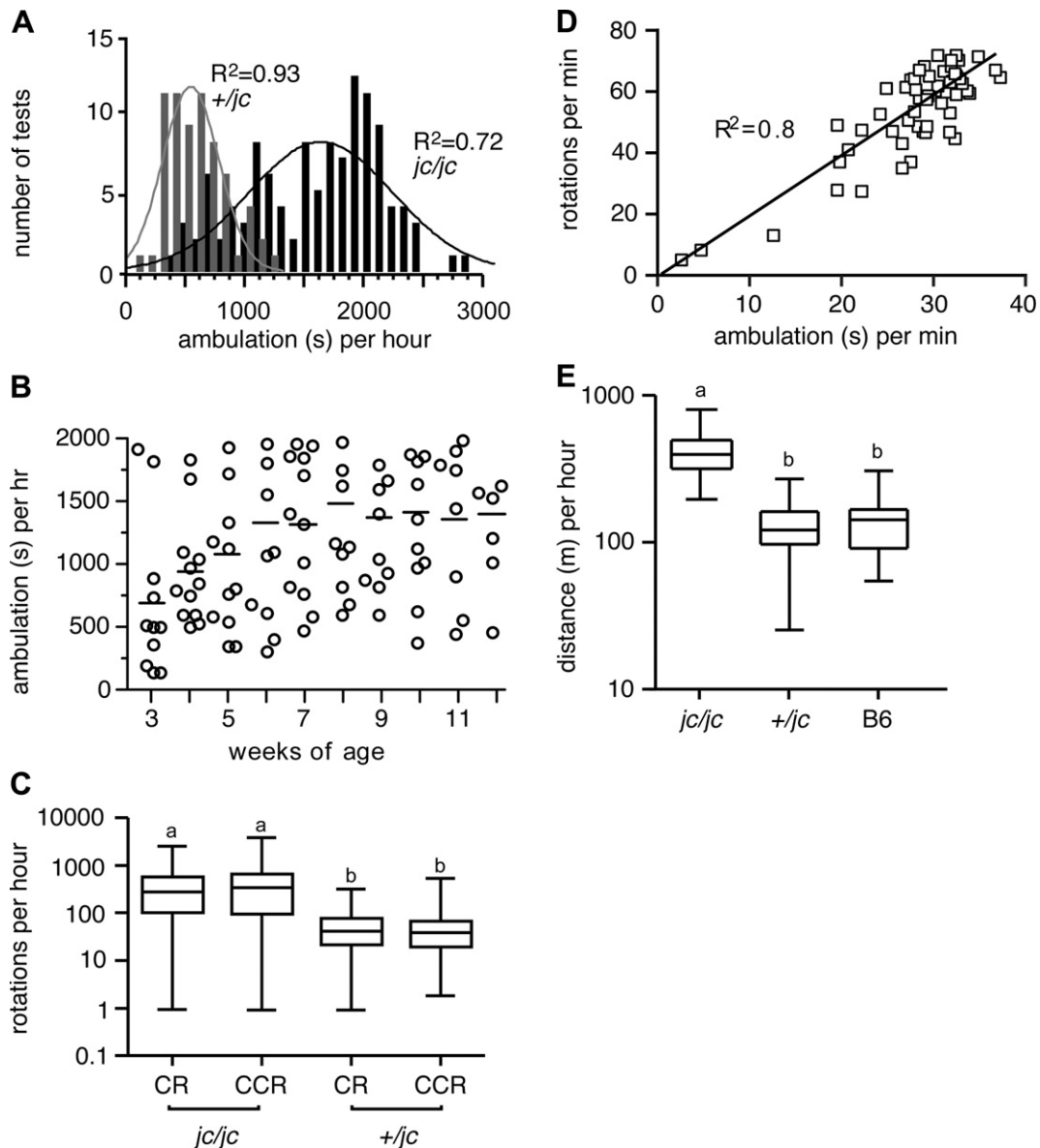


Fig. 1. Open field motor behavior of the *jc* mouse. (A) A histogram of ambulation time of C57BL/6J-+/jc (grey bars) and C57BL/6J-*jc/jc* (black bars) mice is shown. From the heterozygous group, 7 animals six weeks of age or older were tested in a total of 29 tests. From the homozygous group, 22 animals 6 weeks of age or older were tested in a total of 114 tests. The black curves represent the best-fit of a normal distribution and the R^2 values, which indicate the percentage of variation accounted for by the model, are given. (B) The distribution of ambulation time of C57BL/6J-*jc/jc* mice (y -axis) as function of age (x -axis) is summarized. Each circle represents the value obtained for an individual animal and the horizontal line represents the median of the distribution. (C) The distributions of the numbers of clock-wise (CR) and counter-clock wise (CCR) rotations of C57BL/6J-*jc/jc* and C57BL/6J-+/jc mice are shown as box-and-whisker blots, indicating the minimal and maximal value, the 25th and 75th percentile values and the median. Letters annotate significant differences ($p < 0.05$). Test groups were as in A. (D) The correlation between ambulation time (x -axis) and number of rotations (y -axis) is shown for one representative C57BL/6J-*jc/jc* homozygote. The straight line shows the regression curve with the R^2 value as the best-fit parameter. (E) The mean distances traveled by the C57BL/6J-*jc/jc* (test group as in (A)), C57BL/6J-+/jc (test group as in (A)), and C57BL/6J (B6, 45 tests) groups of mice are presented. Distribution of values is given in box-and-whisker plot format.

mutants also exhibited elevated thresholds to 8 kHz, 16 kHz and 32 kHz pure-tone stimuli, and the thresholds increased with increasing frequency. The thresholds varied considerably among the *jc/jc* mutant mice with standard deviations ranging from 7 to 12 dB SPL. Comparison of the threshold means from mutants at 3- to 12-weeks of age did not reveal any age-dependent changes in ABR thresholds over the 10-week test period ($p > 0.05$; Dunnett's multiple comparison

tests). Hearing impairment did not proceed to a complete hearing loss; instead mutants at 22 weeks of age and older had a mean hearing threshold of 93 ± 6 dB SPL ($n = 18$).

The presence of measurable thresholds in the mutants allowed us to determine the latency peak response and inter-peak intervals for peaks I–IV at 90, 95 and 100 dB SPL. Following a 16 kHz tone burst at 100 dB SPL, the first peak (I) appeared with a delay of 1.6 ± 0.13 ms in

Table 1
Movement behavior in *jc*, common inbred strains, and circling mutants

Strains	Age	Ambulation (s)		Distance (m)		Rotations		N/T	
		Mean	SD	Mean	SD	Mean	SD		
C57BL/6J	12–20	676.2	309.0	136.2	52.7	87.5	63.3	4/45	
C3HeB/FeJ	8–16	490.2	172.6	105.1	39.3	129.1	240.9	2/22	
MOLF/Ei	12	481.6	143.5	111.6	41.0	64.1	54.1	2/10	
CZECHII/Ei	12	325.5	119.1	77.6	31.0	47.8	33.5	2/12	
CAST/Ei	4–8	826.3	314.5	215.5	113.6	152.6	94.2	4/10	
C57BL/6J- <i>jc/jc</i>	3	684.8	596.7	167.3	165.4	143.3	189.7	12/12	
	4	940.3	428.9	224.8	127.4	427.4	580.7	12/12	
	5	1073.0	614.2	270.1	190.8	409.5	413.0	12/12	
	6	1321.0	704.3	323.9	195.8	515.3	524.5	12/12	
	7	1312.0	558.9	311.3	154.7	623.8	563.8	12/12	
	8	1471.0	643.2	358.8	186.6	672.8	757.5	12/12	
	9	1369.0	549.5	335.9	161.5	987.0	1420.0	11/11	
	10	1400.0	665.1	345.9	203.2	1032.0	1901.0	11/11	
	11	1350.0	623.3	305.9	152.0	1858.0	1976.0	8/8	
	12	1392.0	585.3	323.9	169.1	621.3	587.9	7/7	
	C57BL/6J-+/ <i>jc</i>	3	344.9	175.9	95.7	65.8	42.7	20.5	4/4
		4	460.9	117.3	94.8	20.0	89.7	90.2	4/4
5		504.5	76.1	120.3	7.0	75.2	15.2	4/4	
6		690.2	260.7	161.4	53.4	160.5	86.4	4/4	
7		546.6	210.3	117.2	48.6	54.0	34.4	4/4	
8		550.7	92.7	120.1	33.7	70.7	29.6	4/4	
9		506.6	69.6	106.5	17.1	62.3	26.9	3/3	
10		513.2	202.5	109.8	43.5	74.0	34.1	3/3	
11		710.0	318.7	143.6	81.7	37.7	31.1	3/3	
12		834.5	192.8	200.7	64.6	156.0	101.8	2/2	
Cdh23 ^{v6J/v6J}		4–16	1811.0	405.8	451.0	124.4	1164.0	960.9	23/59
Cdh23 ^{+v6J}		4–16	580.5	167.5	129.4	44.2	102.2	58.9	23/46
Cdh23 ^{v2J/v2J}	4–16	1675.0	468.6	405.1	14.0	838.5	643.2	18/53	
Cdh23 ^{+v2J}	4–16	730.5	277.6	145.7	53.1	145.0	136.3	13/38	
Myo6 ^{sv/sv}	36	1343.0	487.3	343.1	147.1	675.1	513.3	1/7	
Myo6 ^{+sv}	36	533.3	168.8	114.6	37.6	83.4	40.6	1/7	
Pcdh15 ^{nmf19/nmf19}	16	1887.0	291.9	466.3	99.6	1107.0	599.4	3/17	
Pcdh15 ^{+nmf19}	16	717.7	255.8	152.0	55.6	191.7	239.1	5/31	
Espn ^{je/je}	16–24	1548.0	870.6	344.7	68.6	669.6	596.5	4/36	
Espn ^{+je}	16–24	579.5	277.5	107.6	54.3	108.5	117.7	6/35	
Mcoln3 ^{+VaJ}	8–12	535.1	169.3	115.5	36.7	63.2	40.7	4/10	
Mcoln3 ^{+Va}	48	1812.0	374.6	450.1	127.7	1147.0	773.4	14/49	
Mcoln3 ^{+/+}	48	499.0	137.0	102.9	31.9	99.4	170.8	8/25	
C57BL/6J- <i>jc/jc</i>	3–12	1575.0	486.5	409.0	125.5	985.6	1051.0	20/112	
C57BL/6J-+/ <i>jc</i>	3–12	602.9	239.6	131.6	54.3	116.8	126.6	12/83	
Myo15a ^{sh2/sh2}	4–12	741.6	291.2	167.4	77.2	244.6	411.7	5/25	
Myo15a ^{sh2/sh2}	4–12	1761.0	317.6	474.7	138.1	941.9	384.5	5/38	

Age is given in weeks; s, seconds; SD, standard deviation; m, meter; N/T, number of mice used for number of tests.

mutants ($n = 9$) and 1.6 ± 0.03 ms in heterozygotes ($n = 6$). With decreasing sound pressure levels, the latencies increased while the inter-peak intervals remained constant. There was no statistically significant difference in peak latencies between the mutants and age-matched heterozygous controls (Fig. 2, Table 3).

The *jc*^{2J} homozygotes ($n = 4$) also exhibited elevated hearing thresholds, with the mean threshold for the 16 kHz stimulus being 43 ± 11 dB SPL (Table 2). At the 8 kHz and 16 kHz frequencies, *jc*^{2J} mutants had significantly better hearing than *jc/jc* mice ($p < 0.05$ and $p < 0.001$, respectively, Bonferroni multiple comparison test), but at the click and 32 kHz stimulus hearing was equally poor ($p > 0.05$). Similar to that in the *jc* mice, hear-

ing loss in *jc*^{2J} was not progressive, but rather their hearing thresholds remained stable at 40 dB SPL (16 kHz stimulus) over the 19-week test period (Table 2).

3.3. Distortion-product otoacoustic emissions (DPOAEs) in *jc* mutants

To differentiate the cause of hearing loss, DPOAE function was determined in a cohort of five *+jc* and five *jc/jc* mice at 12-weeks of age. The DPOAEs of heterozygous mice fell within the normal range for all three primary tone levels (55 dB SPL, 65 dB SPL, and 75 dB SPL). In contrast, *jc* homozygotes had no measurable DPOAEs above the noise floor at these primary-tone levels (Fig. 3).

Table 2
ABR thresholds in *jc* and *jc^{2J}* mutants

Cross	Age	Click	8 kHz	16 kHz	32 kHz	N
<i>jc/jc</i>	2	83 ± 11	76 ± 12	90 ± 7	97 ± 5	12
<i>+/jc</i>	2	36 ± 2	20 ± 5	17 ± 3	35 ± 3	10
<i>jc/jc</i>	3	90 ± 12	83 ± 14	91 ± 5	96 ± 6	10
<i>+/jc</i>	3	35 ± 5	24 ± 10	17 ± 7	42 ± 12	12
<i>jc/jc</i>	4	86 ± 10	73 ± 11	83 ± 10	90 ± 7	25
<i>+/jc</i>	4	32 ± 3	25 ± 6	17 ± 6	4 ± 6	10
<i>jc/jc</i>	8	96 ± 5	81 ± 13	86 ± 8	95 ± 6	15
<i>+/jc</i>	8	32 ± 3	23 ± 2	12 ± 3	38 ± 8	7
<i>jc/jc</i>	12	95 ± 6	96 ± 12	86 ± 11	86 ± 8	15
<i>+/jc</i>	12	33 ± 6	25 ± 4	12 ± 5	34 ± 2	6
<i>jc/jc</i>	>22	94 ± 6	87 ± 14	93 ± 6	97 ± 4	18
<i>+/jc</i>	>22	39 ± 2	39 ± 2	26 ± 10	52 ± 4	4
<i>jc^{2J}/jc^{2J}</i>	6	76 ± 7	67 ± 15	43 ± 11	85 ± 15	4
<i>+/jc^{2J}</i>	6	42 ± 4	37 ± 4	15 ± 0	57 ± 4	2
<i>jc^{2J}/jc^{2J}</i>	19	68 ± 9	65 ± 6	41 ± 6	70 ± 0	4

Age is given in weeks; data represent means ± SD; kHz, kilohertz; N, number of animals tested.

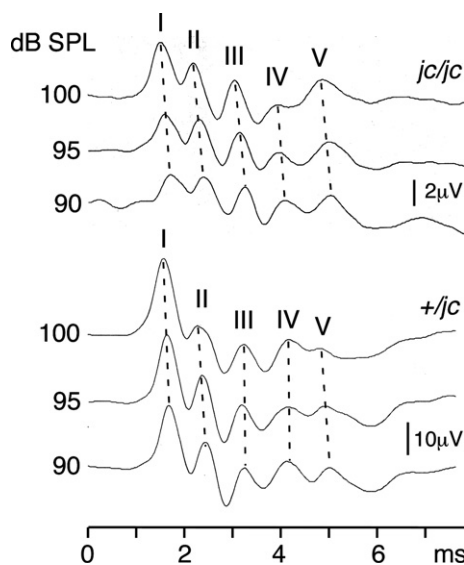


Fig. 2. Auditory-evoked brain stem recording (ABR) waveforms in *jc* mutants. Representative ABRs following a 16 kHz tone-burst at various sound pressure levels (y-axis) in *jc/jc* and *+/jc* mice are shown. The locations of peaks I–V are indicated. Scale bars of the ABRs are given. dB SPL, decibel sound pressure level; ms, millisecond; μ V, microvolt.

3.4. Developmental arrest of cochlear growth

The hearing impairment in the *jc/jc* mutants was accompanied by a structural aberration of the cochlear duct. In *jc*

heterozygotes the cochlea outgrowth developed normally completing the first turn by E15.5 (Fig. 4A and D). In *jc* homozygotes the cochlea duct initially seemed to form normally but at around E13.5 signs of a growth arrest were noticeable (Fig. 4B and C). The truncation became more apparent by E15.5 and an aberrant structure had formed at the apex (Fig. 4E and F). Twenty-six cochleae from 15 *jc/jc* embryos were analyzed and all showed the developmental arrest. Only negligible inter-individual variation in expressivity was observed among the mutants and no laterality effect was noted. In cochleae of 14-day old mutant neonates the apical turn was absent (Fig. 4H and I). No discernable gross abnormalities in the anatomy of the vestibule were seen.

3.5. High-resolution genetic map of *jc*

With the goal of eventually identifying the *jc* gene, the *jc* locus was mapped with high resolution. A total of 1980 chromosomes from an intrasubspecific intercross between C57BL/6J-*jc/jc* and CZECHII/Ei were analyzed with a series of polymorphic markers located within the centromeric half of chromosome 10. Linkage was found between *D10Mit108* and *D10Mit55* (χ^2 test; $p < 0.001$; $df = 1$). Twenty-one recombinant chromosomes were further characterized with newly developed *D10Ntra* markers. The following marker order and distances (centiMorgan ± standard error) were

Table 3
Peak latencies in *+/jc* and *jc/jc* mutants

Cross	dB SPL	I	II	III	IV	V	N
<i>+/jc</i>	100	1.6 ± 0.03	2.4 ± 0.09	3.3 ± 0.10	4.3 ± 0.10	5.2 ± 0.08	6
	95	1.7 ± 0.03	2.5 ± 0.09	3.3 ± 0.07	4.3 ± 0.12	5.2 ± 0.06	6
	90	1.7 ± 0.03	2.5 ± 0.06	3.4 ± 0.08	4.4 ± 0.15	5.3 ± 0.10	6
<i>jc/jc</i>	100	1.6 ± 0.13	2.6 ± 0.42	3.6 ± 0.45	4.5 ± 0.48	5.4 ± 0.38	9
	95	1.7 ± 0.14	2.7 ± 0.43	3.8 ± 0.44	4.6 ± 0.46	5.5 ± 0.34	9
	90	2.1 ± 0.45	3.0 ± 0.68	4.0 ± 0.67	5.0 ± 0.72	5.5 ± 0.32	8

dB SPL, decibel sound pressure level; N, number of animals tested; data represent mean ± SD.

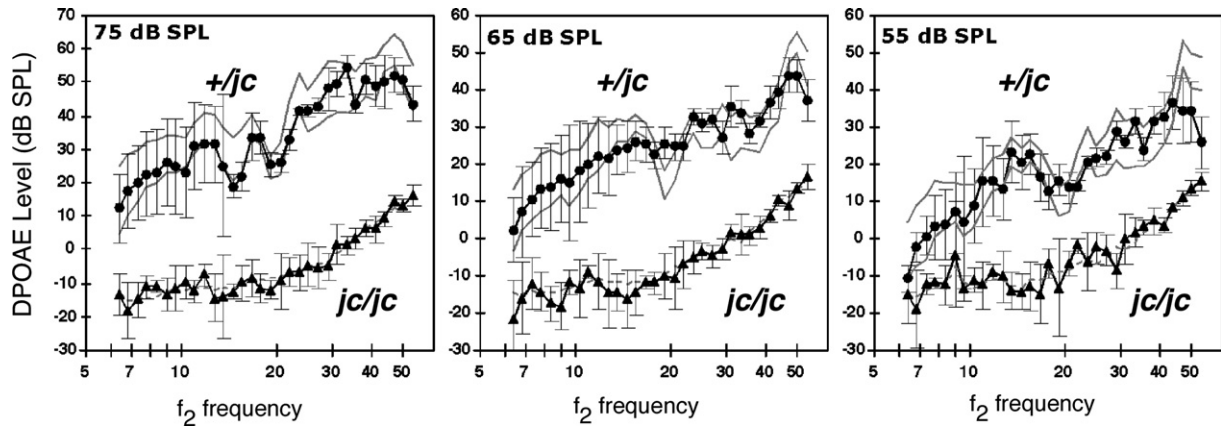


Fig. 3. DPOAEs in *jc* mutants. Average DP-grams ($n = 5$ ears) collected at three primary-tone levels for *+/jc* (solid circles) and *jc/jc* mice (solid triangles) at 3 mo of age. DPOAEs from *+/jc* mice fell in the normal range (± 1 SD) of DPOAEs (solid gray lines) obtained from CBA/CaJ mice known to have normal hearing. DPOAEs from *jc/jc* mice were absent and were at the noise floor of the recording system (dotted gray line). Error bars indicate ± 1 SD.

obtained: *D10Mit108* – 0.05 ± 0.05 – (*D10Ntra116*, *D10Ntra117*) – 0.05 ± 0.05 – *D10Ntra12* – 0.1 ± 0.07 – (*D10Ntra14*, *D10Ntra15*, *jc*) – 0.1 ± 0.07 – (*D10Ntra118*, *D10Ntra119*) – 0.51 ± 0.16 – *D10Ntra111* – 0.05 ± 0.05 – (*D10Ntra114*, *D10Mit55*) (Fig. 5). The *jc* minimal genetic interval was defined by two proximal and two distal recombinations and comprised an interval length of 0.2 ± 0.1 cM. On the mouse physical map (NCBI m34, assembly May 2005), the closest recombinant markers *D10Ntra2* and *D10Ntra16* were separated by a genomic sequence approximately 170 kb in length. This region contained several expressed sequence tags, numerous exons predicted by various gene-prediction algorithms, and multiple cross-species conserved sequences. The human chromosomal region that is homologous to the *jc* minimal genetic interval is present at 6q21. Craniometaphyseal dysplasia (OMIM 218400), which is a recessive syndrome characterized by cranial deformities including hearing loss, is among several human conditions that have been linked to the 6q21 region (Iughetti et al., 2000). However marker *D6S302*, which defines the centromeric border of the linked interval, is located 4 Mb telomeric to the recombinant *jc* marker *D10Ntra118* excluding this syndrome as the human *jc* disease homolog.

The *jc^{2J}* mutation was mapped in a [B6(129S6)-*jc^{2J}*/*jc^{2J}* × CAST/Ei]F1 × F1 intercross. Fifty-three homozygous mutants were genotyped with microsatellite markers and the following map location was obtained: *D10Mit80* – 1.7cM – (*D10Mit55*, *jc^{2J}*) – 3cM – *D10Mit138* (Fig. 5). To formally test for allelism, heterozygous *+/jc^{2J}* mice were crossed with C57BL/6J-*jc/jc* mutants; three out of eight animals produced by this cross showed the circling and hearing impairment phenotype that is characteristic of the *jc* mutant.

3.6. ABR threshold distributions on different genetic backgrounds

Hearing thresholds on the C57BL/6J coisogenic background showed a characteristic variation, such that at an

average age of eleven weeks a cohort of 67 C57BL/6J-*jc/jc* mutants had a mean ABR threshold of 90 ± 9 dB SPL. The lowest threshold measured was 60 dB SPL, but most of the thresholds (≥ 25 th percentile) were equal to or higher than 85 dB SPL (Fig. 6A, Table 4). On both CAST/Ei and CZECHII/Ei genetic backgrounds hearing thresholds of *jc/jc* mutants were significantly lower than that on the C57BL/6J background ($p < 0.01$; Dunnett's multiple comparison test). In particular, F2 homozygotes ($n = 80$) from a (C57BL/6J-*jc/jc* × CAST/Ei) F1 intercross and F2 homozygotes ($n = 48$) from a (C57BL/6J-*jc/jc* × CZECHII/Ei) F1 intercross had thresholds of 55 ± 13 dB SPL and 62 ± 22 dB SPL, respectively. Hearing thresholds in both the B6/CAST-*jc/jc* and B6/CZECH-*jc/jc* F2 populations followed a normal distribution ($p = 0.8$ and $p = 0.1$, respectively; D'Agostino and Pearson test) (Fig. 6B and C). Hearing thresholds in *jc* homozygotes ($n = 43$) obtained from a [(C57BL/6J-*jc/jc* × CZECHII/Ei) F1 × C57BL/6J-*jc/jc*] backcross were also significantly lower ($p < 0.01$) than those of *jc* homozygotes on the isogenic background. Thresholds, however, were not normally distributed ($p = 0.0002$), but instead showed a bi-modal scatter, with the first tier comprising thresholds from 15 to 50 dB SPL ($n = 17$) and the second tier containing thresholds from 60 to 95 dB SPL ($n = 26$). The ratio between these two groups was 1:1.5. (Fig. 6D). Interestingly, the genetic background did not affect the degree of the cochlea dysplasia (data not shown). To test whether thresholds would distribute into discrete groups over time, *jc* homozygotes from the normal hearing spectrum were tested at older ages. Consistent with the observation in mice on the isogenic background, age had no effect on the thresholds in these intercross progeny (data not shown).

3.7. Genome wide linkage scan

The lower thresholds observed in the progeny of the outcrosses and the differing distributions observed in the

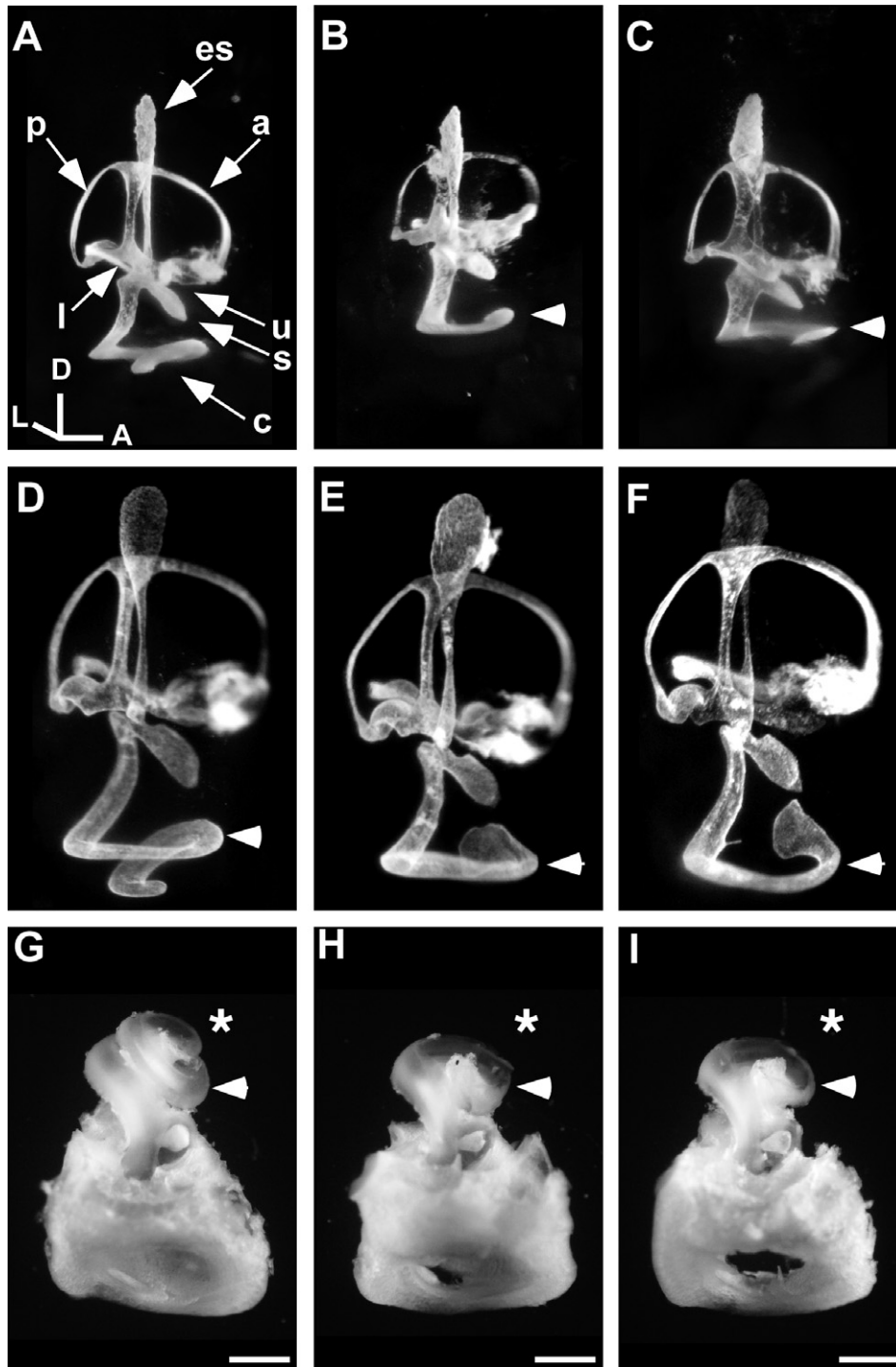


Fig. 4. Cochlea malformation in *jc* mutants. Pictures (A)–(F) show paint-fills of the inner ear's membranous labyrinth. Ears shown in (A)–(C) were obtained from E13.5 day old embryos and ears shown in (D)–(F) were from E15.5 day old embryos. Pictures (G)–(I) show inner ears from 14-day old neonates in which the temporal bone was removed to expose the cochlea duct. Two mutant ears are shown per time point. Ears shown in A, D, and G were obtained from *+l/jc* mice and ears shown in B, C, E, F, H, and I were obtained from *jc/jc* mutants. To aid in phenotype classification ears from the progeny of *jc/jc* × *jc/jc* matings were included in the study. Arrowheads point to the upper cochlea turn. Asterisks indicate the missing apical turn. c, cochlea duct; s, sacculus; u, utricle; es, endolymphatic sac, l, lateral; a, anterior, p, posterior semicircular canal; scale bar in G, H, and I equals 0.5 mm.

progeny of the intercrosses and the backcross led to the hypothesis that dominant alleles contributed by the CAST/Ei and CZECHIII/Ei strains partially restored hearing in the outcrossed homozygous mutants. To test this proposi-

tion, genome-wide linkage analyses were conducted. Forty-two B6/CZECH-*jc/jc* backcross progeny, representing 98% of the *jc/jc* N2 population, were genotyped at 137 marker loci. Marker regression analyses identified a significant

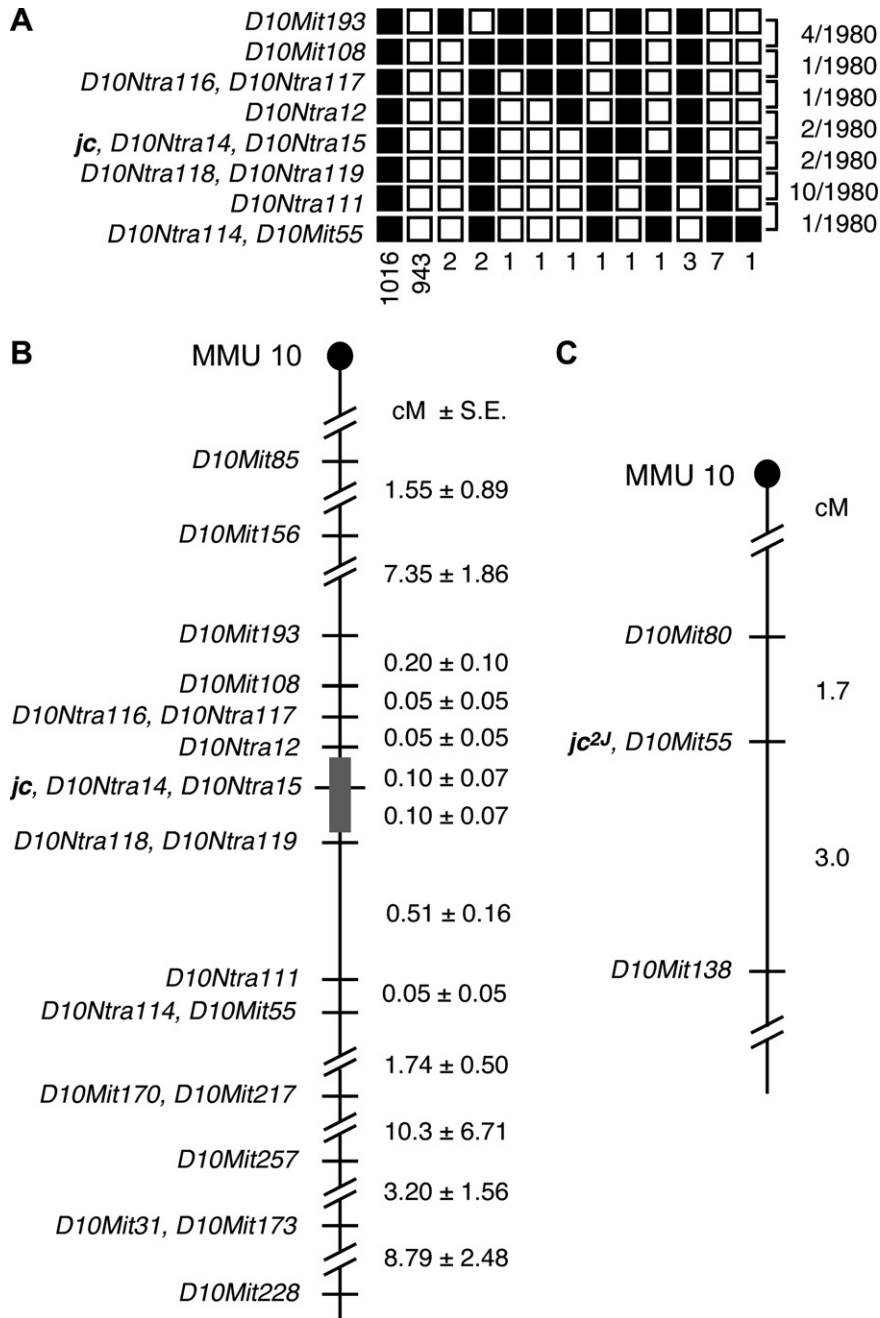


Fig. 5. Genetic map and haplotype of the *jc* locus at chromosome 10. (A) The haplotype distribution in the F2 population is shown. Polymorphic markers are indicated on the left, numbers of recombinations per total meioses are given on the right and haplotype frequencies are shown at the bottom. Black boxes indicate alleles of the *jc* chromosome and the white boxes indicate the CZECHII/Ei-derived allele. (B) The marker locations on proximal chromosome 10 (MMU Chr10) are shown. Marker order is shown on the left and genetic distances are given on the right. The *jc* critical interval is highlighted. (C) The chromosomal location of the *jc^{2j}* locus is shown. Markers are given on the left and marker distances (in cM) are given on the right.

QTL associated with marker *D18Mit60* (position 16cM) with LOD scores of 3.1 and 3.5 (significance threshold: 3.1) for the 8 kHz and 16 kHz stimuli, respectively. Pairwise marker regression analyses to test for interacting loci revealed no significant association (Table 5). Forty-five B6/CZECH-*jc/jc* F2 progeny (representing 94% of the *jc/jc* F2 population) were genotyped at 143 marker loci. Significant genome-wide linkage was found with the 8 kHz

and 16 kHz traits at *D9Mit151* (position 72cM) with LOD scores of 5.5 and 4.8, respectively (Table 5). The B6/CAST-*jc/jc* F2 offspring were scanned using a selective genotyping protocol. Twenty-one F2 progeny from the lower ≤25th percentile range (hearing threshold range: 15 dB SPL – 45 dB SPL) and nineteen F2 progeny from 68 to 97th percentile range (hearing threshold range: 65 dB SPL – 95 dB SPL) were genotyped at 127 marker

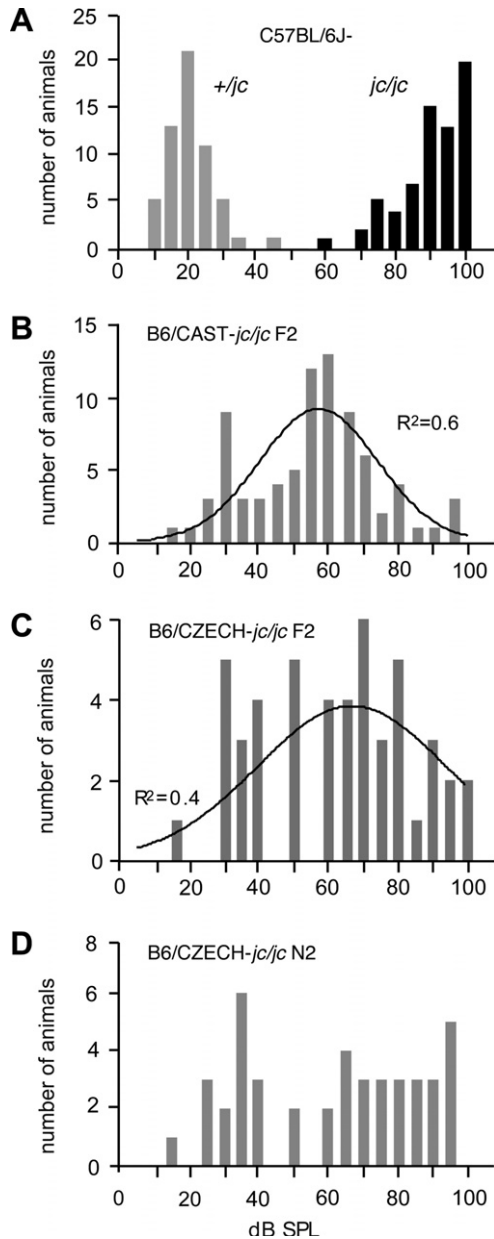


Fig. 6. ABR threshold distributions of *jcljc* homozygotes on different genetic backgrounds. Shown in (A) is the histogram of hearing thresholds for the 16 kHz tone-burst stimulus in C57BL/6J-+/jc (grey bars) and C57BL/6J-*jcljc* (black bars) mice. Shown in B and C are the histograms of hearing threshold distributions of *jcljc* homozygotes from the (CAST/Ei × C57BL/6J-*jcljc*) F1 × F1 intercross and the (CZECHII/Ei × C57BL/6J-*jcljc*) F1 × F1 intercross, respectively. The best-fit curves for a Gaussian distribution are shown as solid black curves. The regression coefficient for the curve is given as R^2 . Shown in D is the histogram of hearing thresholds of *jcljc* homozygotes from the (CZECHII/Ei × C57BL/6J-*jcljc*) × C57BL/6J-*jcljc* backcross. For (A)–(D) the horizontal axis denotes hearing thresholds in decibel sound pressure levels (dB SPL) and the vertical axis gives the number of animals.

loci. One marker on chr 12 (*D12Mit172*) showed suggestive linkage with a LOD score of 5.0 (significance threshold: 2.9) at the 16 kHz stimulus. The click, 8 kHz and 32 kHz stimuli showed no linkage. Pair-wise marker regression

analyses to test for interacting loci revealed no significant association.

3.8. Advanced backcross lines

To further test the hypothesis that dominant modifier alleles reduced hearing thresholds in the outcrossed homozygotes, two segregating lines were generated. Through repeated backcrossing of F2 and N2 B6/CZECH-*jcljc* homozygotes with the lowest thresholds at the 16 kHz stimulus to C57BL/6J-+/jc heterozygotes we expected to isolate the CZECH-derived genomic segment(s) that are responsible for the lower thresholds. At generation N5, *jcljc* homozygotes with the lowest (30 dB SPL at 16 kHz) and highest thresholds (95 dB SPL) from each of the two independent backcross lines were genotyped at 137 marker loci to identify common CZECH-derived chromosomal segments. As expected each of the two lines segregated a unique set of genomic segments (six and eight) from the donor strain; segments from chromosomes 2, 3, and 11 were segregating in both lines. Additional N5 progeny from both lines ($n = 28$, Fig. 7) were genotyped to correlate the congenic intervals with hearing status. None of the congenic intervals from either line showed a clear correlation with hearing status (ANOVA) and appeared to be randomly assorted among the normal and hearing-impaired N5 *jcljc* homozygotes.

We next backcrossed a *jcljc* homozygote of the N7 generation with a 100 dB SPL threshold (not expected to carry modifying CZECH-alleles) with a C57BL/6J-+/jc mouse. Unexpectedly, we recovered *jcljc* homozygotes with hearing thresholds in the 40–50 dB SPL range. The hearing thresholds for this N8 control group did not differ from that of the test groups of the N3–N7 generations (ANOVA; $p > 0.05$) (Fig. 7).

4. Discussion

4.1. Cochlea malformation

In this study, we identified several features that are characteristic of the Jackson circler phenotype. Perhaps the most interesting finding was the observation that *jc* mutants showed a response, albeit abnormal, to acoustic stimuli at a young age and preserved this residual hearing over an extended period of time. This hearing retention is in contrast to the phenotypes observed for many spontaneous deafness waltzing mutants, which are either congenitally deaf or show a rapid decline in hearing function after birth. The hearing at high sound pressure levels in coisogenic *jc* mutants was characterized by a scattering of thresholds at all stimuli, which suggests that cochlea function in *jc* is prone to stochastic effects. The absence of DPOAEs at the primary-tone levels of 55, 65, and 75 dB SPL was consistent with the absence of ABR thresholds at the corresponding stimuli and suggests that dysfunction of outer hair cells may underlie the hearing deficit. The

Table 4
ABR thresholds of *jc/jc* homozygotes

Cross		Click	8 kHz	16 kHz	32 kHz
C57BL/6J- <i>jc/jc</i>	<i>N</i>	69	69	69	68
	Mean	93.5	85.1	89.4	97.0
	SD	8.3	13.1	9.3	5.6
C57BL/6J-+/ <i>jc</i>	<i>N</i>	32	32	32	32
	Mean	33.9	25.8	21.1	37.7
	SD	7.3	8.7	8.3	7.8
B6/CZECH- <i>jc/jc</i> F2	<i>N</i>	49	49	48	44
	Mean	72.4	58.8	61.8	79.9
	SD	11.3	21.1	22.0	16.1
B6/CAST- <i>jc/jc</i> F2	<i>N</i>	82	81	80	74
	Mean	70.4	54.2	55.1	75.6
	SD	12.6	15.4	18.3	14.3
B6/CZECH- <i>jc/jc</i> N2	<i>N</i>	44	43	43	43
	Mean	75.3	55.8	61.3	78.1
	SD	14.3	21.0	24.7	20.2

N, number of animals tested; SD, standard deviation; kHz, kilohertz.

residual hearing may be mediated by still functioning inner hair cells. The comparison of ABR thresholds showed that *jc^{2J}* mutants had significantly better hearing than *jc* homozygotes of a similar age. Thus it may be that the *jc^{2J}* allele is less severe than the *jc* allele.

ABR waves are thought to originate in the cochlea (peak I) and from brainstem nuclei including the cochlea nucleus (peaks II and III), medial superior olivary nuclei (peak IV), and nuclei in the inferior colliculus (peak V) (Melcher and Kiang, 1996a; Melcher et al., 1996b; Melcher et al., 1996c). Myelin-deficiency of auditory nerve fibers in trembler mice (*Pmp22^{Tr-J}*) were recently shown to result in a prolonged peak I latency (Zhou et al., 1995a; Zhou et al., 1995b). The peak-latencies measured in the *jc* mutants were comparable to that seen in the heterozygotes, indicating that the main generators of the ABR were functioning properly. The peak latency of 1.7 ± 0.03 ms seen with 90 dB SPL stimuli in +/*jc* heterozygotes also correlated well with the 1.6 ms latency recorded in one-month-old C57BL/6J mice (Hunter and Willott, 1987).

The altered ABR phenotype of the mutants correlated with a marked morphogenetic defect of the cochlea. Similarly truncated cochleae were observed in mutant alleles of genes that are known to be involved in patterning pathways such as *Pax2*, *Eya1*, *Ltap1*, and *Dvl2* (Curtin et al., 2003; Johnson et al., 1999; Montcouquiol et al., 2003; Tor-

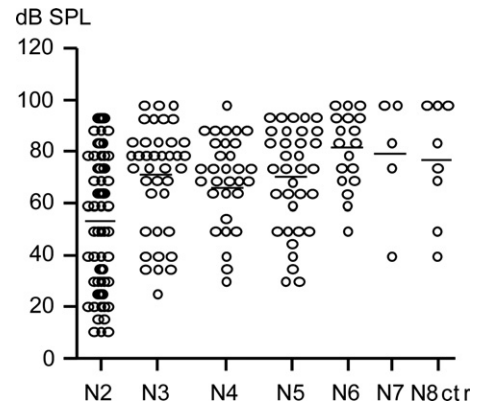


Fig. 7. ABR threshold distribution as a function of backcross generation. Hearing thresholds for the 16 kHz stimulus in *jc/jc* homozygous backcross progeny at the indicated backcross generation (N2–N7) are shown. Each circle represents the threshold in dB SPL of one animal. The horizontal black line indicates the mean of the population. The threshold means in the advanced backcross lines (generation N3–N7) ranged from 71 dB SPL to 80 dB SPL and did not differ significantly ($p > 0.05$; Bonferroni's multiple comparison test). N8 ctr, control group at generation N8.

res et al., 1996; Wang et al., 2005; Xu et al., 1999). Although the deafness waltzing phenotype initially seemed to be indicative of a type of degenerative process within the organ of Corti, the paint-filling data suggest the *jc* gene has a function in the growth and extension of the cochlear coil during development.

The cochlea malformation seen in the *jc* mutant mouse is reminiscent of Mondini deformity in humans, which was first described by Carlo Mondini in 1791 who reported missing apical turns in both cochleae of a deaf boy (Mondini, 1997; Mundinus, 1791). Nowadays, Mondini dysplasia comprises a spectrum of morphological aberrations in the inner ear that include aplastic cochlea, enlarged vestibular aqueduct (EVA) and other deformations of the bony and membranous labyrinth. Clinical and molecular studies correlated EVA and Mondini dysplasia with Pendred syndrome (MIM 274600) and mutations of the pendrin gene *SLC26A4* (Campbell et al., 2001; Pryor et al., 2005; Tsukamoto et al., 2003; Usami et al., 1999). Not all cases of non-syndromic EVA were accounted for by mono- and diallelic mutations in *SLC26A4* suggesting that mutations in other loci may cause non-syndromic EVA or modify mutant *SLC26A4* alleles (Pryor et al., 2005; Tsukamoto et al., 2003; Usami et al., 1999). The *Slc12a2* gene, which shows motif similarities to *Slc26a4* and also underlies

Table 5
Summary of the mapping statistic

Cross	Trait	Marker	LOD	%	CI	Add
B6/CZECH- <i>jc/jc</i> N2	8 kHz	<i>D18Mit60</i>	3.2	29	43	–22.71
	16 kHz	<i>D18Mit60</i>	3.5	32	40	–27.99
B6/CZECH- <i>jc/jc</i> F2	8 kHz	<i>D9Mit151</i>	5.5	43	27	–14.49
	16 kHz	<i>D9Mit151</i>	4.8	39	30	–13.62

%, Percent variation explained by marker locus; CI, 95% percent confidence interval; regression coefficient.

deafness in the shaker-with-syndactylism mutant (sy^{fp}) is a good candidate for such a second locus, but jc might also be involved in EVA and Mondini dysplasia (Delpire et al., 1999; Dixon et al., 1999; Flagella et al., 1999). However, despite the gross-morphological similarities with Mondini dysplasia, our paint-filling studies did not reveal a significantly enlarged endolymphatic duct in the mutants at E15.5. Instead, compared with the dilated endolymphatic duct and vestibule at E15.5–16.5 seen in *Slc26a4*-deficient mice (Everett et al., 2001), the membranous labyrinth in jc mutants appeared fairly normal. It is possible however that a dilation or enlargement of the endolymphatic duct in jc mutants may occur later in development.

4.2. Erratic circling behavior

Ambulatory and circling behavior of jc mice was ascertained by quantifying movements in an open field. Consistent with the previous observation that circling becomes more pronounced with age (Southard, 1970) we found that three to five week-old homozygotes with normal ambulation times developed abnormal movement behavior by six weeks of age. As expected for a behavioral trait, we also found a wide scatter of data points and means with large standard deviations. Despite this variability, there were clear differences between the test groups that included common laboratory and wild-derived strains and jc homozygotes. Jones and colleagues recently assessed gravity receptor function by measuring vestibular-evoked potentials (VsEPs) in a series of mutants including the Jackson circler (Jones et al., 2005). No response could be elicited in six-week old jc mice ($n = 5$) suggesting a pathology in sensory hair cells of saccule and utricle (Jones et al., 2005).

To further distinguish the vestibular abnormality, a panel of circling mutants was included in the study. All of the panel's mutants had a known pathology in the vestibular neuroepithelium (Deol, 1954; Di Palma et al., 2001; Sjöstrom and Anniko, 1990), with the exception of *Pcdh15^{aw}* (Alagramam et al., 2005). Under our test conditions, ambulation time and circling behavior was indistinguishable among the different mutant strains. Clearly, this was due, at least in part, to the presence of similar defects in the vestibule. Considered together with the results obtained by Jones and colleagues these data suggest that a primary defect in the vestibular neuroepithelium was the cause of the circling behavior. Interestingly, Löscher and colleagues recently found that altered rate and discharge patterns in basal ganglia neurons correlated with circling and hyperactivity behavior in the *ci2* rat mutant (Fedrowitz et al., 2003; Kaiser et al., 2001). Besides the central and behavioral phenotypes, *ci2* rats are deaf due to degeneration of the organ of Corti but show a normal vestibular neuroepithelium, similar to the Ames waltzer mouse mutant (Alagramam et al., 2005). It may be that likewise affected central pathways contribute to the abnormal movement behavior in jc mice.

4.3. Hearing thresholds and genetic background

Expression of the Jackson circler phenotype was highly dependent upon the genetic background. A significant variability of hearing thresholds was already observed on the C57BL/6J isogenic strain, which may indicate that jc is not a complete loss-of-function allele. On both the CAST/Ei and CZECHII/Ei background, hearing thresholds in jc homozygotes were widely distributed, and in some instances the hearing loss was completely rescued. The large threshold shift towards the normal hearing range in the F2 and N2 progeny and the differing distribution in the backcross versus the intercross strongly argue that genetic factors control this distribution. In the B6/CZECH- jc backcross and B6/CZECH- jc intercross, significant linkage was obtained with markers on chromosome 18 and 9, respectively. However these marker alleles were inversely correlated with hearing thresholds in both crosses, such that lower thresholds were associated with C57BL/6J-derived alleles and not with CZECH-alleles as expected. In addition, phenotype-based backcrossing was unsuccessful in isolating a genomic segment that could be linked unambiguously with better hearing, although we were able to clearly identify and segregate the trait. While many quantitative traits can be mapped with genome-wide significant LOD scores, isolating the congenic intervals and identifying the quantitative trait nucleotide(s) (QTNs) has proven to be much more difficult (Flint et al., 2005; Legare et al., 2000). In cases where hearing loss QTNs and hearing modifiers were molecularly identified, the locus accounted for a significant portion of the overall variance and could also be interpreted as a Mendelian trait with reduced penetrance (Ikeda et al., 1999; Noben-Trauth et al., 1997). In our study, it is possible that numerous small-effect modifier genes controlled the variation in the F2 and N2 crosses, which could not be detected due to the limited sample size. The lower thresholds in the advanced backcross generations, are probably due to stochastic effects, which we also observed in jc homozygotes in the C57BL/6J background.

Acknowledgements

The authors thank Melissa Irby and Jimmy Fiallos for technical assistance, ABR measurements, open-field testing, and maintenance of the mouse colonies. We thank Doris Wu for help with the paint fillings. We thank Doris Wu and Matt Kelley for reading the manuscript. This work was supported by the Intramural Research Program at NIDCD/NIH (K.N.T.), DC000613 and DC003114 to GKM and DC04301 to K.R.J.

References

- Alagramam, K.N., Stahl, J.S., Jones, S.M., Pawlowski, K.S., Wright, C.G., 2005. Characterization of vestibular dysfunction in the mouse model for Usher syndrome 1F. *J. Assoc. Res. Otolaryngol.* 6, 106–118.

- Campbell, C., Cucci, R.A., Prasad, S., Green, G.E., Edeal, J.B., Galer, C.E., Karniski, L.P., Sheffield, V.C., Smith, R.J., 2001. Pendred syndrome, DFNB4, and PDS/SLC26A4 identification of eight novel mutations and possible genotype-phenotype correlations. *Hum. Mutat.* 17, 403–411.
- Churchill, G.A., Doerge, R.W., 1994. Empirical threshold values for quantitative trait mapping. *Genetics* 138, 963–971.
- Cordes, S.P., Barsh, G.S., 1994. The mouse segmentation gene *kr* encodes a novel basic domain-leucine zipper transcription factor. *Cell* 79, 1025–1034.
- Curtin, J.A., Quint, E., Tshipouri, V., Arkell, R.M., Cattanch, B., Copp, A.J., Henderson, D.J., Spurr, N., Stanier, P., Fisher, E.M., Nolan, P.M., Steel, K.P., Brown, S.D., Gray, I.C., Murdoch, J.N., 2003. Mutation of *Celsr1* disrupts planar polarity of inner ear hair cells and causes severe neural tube defects in the mouse. *Curr. Biol.* 13, 1129–1133.
- Delpire, E., Lu, J., England, R., Dull, C., Thorne, T., 1999. Deafness and imbalance associated with inactivation of the secretory Na-K-2Cl co-transporter. *Nat. Genet.* 22, 192–195.
- Deol, M.S., 1954. The anomalies of the labyrinth of the mutants varitint-waddler, shaker-2 and jerker in the mouse. *J. Genet.* 52, 562–588.
- Di Palma, F., Holme, R.H., Bryda, E.C., Belyantseva, I.A., Pellegrino, R., Kachar, B., Steel, K.P., Noben-Trauth, K., 2001. Mutations in *Cdh23*, encoding a new type of cadherin, cause stereocilia disorganization in waltzer, the mouse model for Usher syndrome type 1D. *Nat. Genet.* 27, 103–107.
- Dixon, M.J., Gazzard, J., Chaudhry, S.S., Sampson, N., Schulte, B.A., Steel, K.P., 1999. Mutation of the Na-K-Cl co-transporter gene *Slc12a2* results in deafness in mice. *Hum. Mol. Genet.* 8, 1579–1584.
- Eppig, J.T., Bult, C.J., Kadin, J.A., Richardson, J.E., Blake, J.A., Anagnostopoulos, A., Baldarelli, R.M., Baya, M., Beal, J.S., Bello, S.M., Boddy, W.J., Bradt, D.W., Burkart, D.L., Butler, N.E., Campbell, J., Cassell, M.A., Corbani, L.E., Cousins, S.L., Dahmen, D.J., Dene, H., Diehl, A.D., Drabkin, H.J., Frazer, K.S., Frost, P., Glass, L.H., Goldsmith, C.W., Grant, P.L., Lennon-Pierce, M., Lewis, J., Lu, I., Maltais, L.J., McAndrews-Hill, M., McClellan, L., Miers, D.B., Miller, L.A., Ni, L., Ormsby, J.E., Qi, D., Reddy, T.B., Reed, D.J., Richards-Smith, B., Shaw, D.R., Sinclair, R., Smith, C.L., Szauter, P., Walker, M.B., Walton, D.O., Washburn, L.L., Witham, I.T., Zhu, Y., 2005. The mouse genome database (MGD): from genes to mice – a community resource for mouse biology. *Nucleic Acids Res.* 33, D471–D475.
- Everett, L.A., Belyantseva, I.A., Noben-Trauth, K., Cantos, R., Chen, A., Thakkar, S.I., Hoogstraten-Miller, S.L., Kachar, B., Wu, D.K., Green, E.D., 2001. Targeted disruption of mouse *Pds* provides insight about the inner-ear defects encountered in Pendred syndrome. *Hum. Mol. Genet.* 10, 153–161.
- Fedrowitz, M., Lindemann, S., Loscher, W., Gernert, M., 2003. Altered spontaneous discharge rate and pattern of basal ganglia output neurons in the circling (*ci2*) rat mutant. *Neuroscience* 118, 867–878.
- Flagella, M., Clarke, L.L., Miller, M.L., Erway, L.C., Giannella, R.A., Andringa, A., Gawenis, L.R., Kramer, J., Duffy, J.J., Doetschman, T., Lorenz, J.N., Yamoah, E.N., Cardell, E.L., Shull, G.E., 1999. Mice lacking the basolateral Na-K-2Cl cotransporter have impaired epithelial chloride secretion and are profoundly deaf. *J. Biol. Chem.* 274, 26946–26955.
- Flint, J., Valdar, W., Shifman, S., Mott, R., 2005. Strategies for mapping and cloning quantitative trait genes in rodents. *Nat. Rev. Genet.* 6, 271–286.
- Hasson, T., Heintzelman, M.B., Santos, S.J., Corey, D.P., Mooseker, M.S., 1995. Expression in cochlea and retina of myosin VIIa, the gene product defective in Usher syndrome type 1B. *Proc. Natl. Acad. Sci. USA* 92, 9815–9819.
- Hequembourg, S., Liberman, M.C., 2001. Spiral ligament pathology: a major aspect of age-related cochlear degeneration in C57BL/6 mice. *J. Assoc. Res. Otolaryngol.* 2, 118–129.
- Hunter, K.P., Willott, J.F., 1987. Aging and the auditory brainstem response in mice with severe or minimal presbycusis. *Hear. Res.* 30, 207–218.
- Ikeda, A., Zheng, Q.Y., Rosenstiel, P., Maddatu, T., Zuberi, A.R., Roopenian, D.C., North, M.A., Naggert, J.K., Johnson, K.R., Nishina, P.M., 1999. Genetic modification of hearing in tubby mice: evidence for the existence of a major gene (*moth1*), which protects tubby mice from hearing loss. *Hum. Mol. Genet.* 8, 1761–1767.
- Iughetti, P., Alonso, L.G., Wilcox, W., Alonso, N., Passos-Bueno, M.R., 2000. Mapping of the autosomal recessive (AR) craniometaphyseal dysplasia locus to chromosome region 6q21-22 and confirmation of genetic heterogeneity for mild AR spondylocostal dysplasia. *Am. J. Med. Genet.* 95, 482–491.
- Jimenez, A.M., Stagner, B.B., Martin, G.K., Lonsbury-Martin, B.L., 1999. Age-related loss of distortion product otoacoustic emissions in four mouse strains. *Hear. Res.* 138, 91–105.
- Jimenez, A.M., Stagner, B.B., Martin, G.K., Lonsbury-Martin, B.L., 2001. Susceptibility of DPOAEs to sound overexposure in inbred mice with AHL. *J. Assoc. Res. Otolaryngol.* 2, 233–245.
- Johnson, K.R., Cook, S.A., Erway, L.C., Matthews, A.N., Sanford, L.P., Paradies, N.E., Friedman, R.A., 1999. Inner ear and kidney anomalies caused by IAP insertion in an intron of the *Eya1* gene in a mouse model of BOR syndrome. *Hum. Mol. Genet.* 8, 645–653.
- Johnson, K.R., Zheng, Q.Y., Noben-Trauth, K., 2006. Strain background effects and genetic modifiers of hearing in mice. *Brain Res.* 1091, 79–88.
- Jones, S.M., Johnson, K.R., Yu, H., Erway, L.C., Alagramam, K.N., Pollak, N., Jones, T.A., 2005. A quantitative survey of gravity receptor function in mutant mouse strains. *J. Assoc. Res. Otolaryngol.*, 1–14.
- Kaiser, A., Fedrowitz, M., Ebert, U., Zimmermann, E., Hedrich, H.J., Wedekind, D., Loscher, W., 2001. Auditory and vestibular defects in the circling (*ci2*) rat mutant. *Eur. J. Neurosci.* 14, 1129–1142.
- Keithley, E.M., Canto, C., Zheng, Q.Y., Fischel-Ghodsian, N., Johnson, K.R., 2004. Age-related hearing loss and the *ahl* locus in mice. *Hear. Res.* 188, 21–28.
- Lander, E., Kruglyak, L., 1995. Genetic dissection of complex traits: guidelines for interpreting and reporting linkage results. *Nat. Genet.* 11, 241–247.
- Legare, M.E., Bartlett 2nd, F.S., Frankel, W.N., 2000. A major effect QTL determined by multiple genes in epileptic EL mice. *Genome Res.* 10, 42–48.
- Manly, K.F., Cudmore Jr., R.H., Meer, J.M., 2001. Map Manager QTX, cross-platform software for genetic mapping. *Mamm. Genome* 12, 930–932.
- Martin, P., Swanson, G.J., 1993. Descriptive and experimental analysis of the epithelial remodellings that control semicircular canal formation in the developing mouse inner ear. *Dev. Biol.* 159, 549–558.
- Mburu, P., Mustapha, M., Varela, A., Weil, D., El-Amraoui, A., Holme, R.H., Rump, A., Hardisty, R.E., Blanchard, S., Coimbra, R.S., Perfettini, I., Parkinson, N., Mallon, A.M., Glenister, P., Rogers, M.J., Paige, A.J., Moir, L., Clay, J., Rosenthal, A., Liu, X.Z., Blanco, G., Steel, K.P., Petit, C., Brown, S.D., 2003. Defects in whirler, a PDZ domain molecule involved in stereocilia elongation, cause deafness in the whirler mouse and families with DFNB31. *Nat. Genet.* 34, 421–428.
- Melcher, J.R., Kiang, N.Y., 1996a. Generators of the brainstem auditory evoked potential in cat. III: Identified cell populations. *Hear. Res.* 93, 52–71.
- Melcher, J.R., Guinan Jr., J.J., Knudson, I.M., Kiang, N.Y., 1996b. Generators of the brainstem auditory evoked potential in cat. II. Correlating lesion sites with waveform changes. *Hear. Res.* 93, 28–51.
- Melcher, J.R., Knudson, I.M., Fullerton, B.C., Guinan Jr., J.J., Norris, B.E., Kiang, N.Y., 1996c. Generators of the brainstem auditory evoked potential in cat. I. An experimental approach to their identification. *Hear. Res.* 93, 1–27.
- MGD. 2005. Mouse Genome Informatics Project, The Jackson Laboratory, Bar Harbor, ME. World Wide Web (URL: <http://www.informatics.jax.org>).
- Mondini, C., 1997. Minor works of Carlo Mondini: the anatomical section of a boy born deaf. *Am. J. Otol.* 18, 288–293 (Translation).

- Montcouquiol, M., Rachel, R.A., Lanford, P.J., Copeland, N.G., Jenkins, N.A., Kelley, M.W., 2003. Identification of *Vangl2* and *Scrib1* as planar polarity genes in mammals. *Nature* 423, 173–177.
- Mundinus, C., 1791. *Opuscula Caroli Mundini: Anatomica surdi natio sectio. De Bononiensi Scientarium et Artium atque Academia Commentarii*. 7.
- Nadeau, J.H., 2001. Modifier genes in mice and humans. *Nat. Rev. Genet.* 2, 165–174.
- Nadeau, J.H., 2003. Modifier genes and protective alleles in humans and mice. *Curr. Opin. Genet. Dev.* 13, 290–295.
- Noben-Trauth, K., Zheng, Q.Y., Johnson, K.R., Nishina, P.M., 1997. *mdfw*: a deafness susceptibility locus that interacts with deaf waddler (*dfw*). *Genomics* 44, 266–272.
- Phippard, D., Lu, L., Lee, D., Saunders, J.C., Crenshaw 3rd, E.B., 1999. Targeted mutagenesis of the POU-domain gene *Brn4/Pou3f4* causes developmental defects in the inner ear. *J. Neurosci.* 19, 5980–5989.
- Pryor, S.P., Madeo, A.C., Reynolds, J.C., Sarlis, N.J., Arnos, K.S., Nance, W.E., Yang, Y., Zalewski, C.K., Brewer, C.C., Butman, J.A., Griffith, A.J., 2005. *SLC26A4/PDS* genotype-phenotype correlation in hearing loss with enlargement of the vestibular aqueduct (EVA): evidence that Pendred syndrome and non-syndromic EVA are distinct clinical and genetic entities. *J. Med. Genet.* 42, 159–165.
- Quint, E., Steel, K., 2003. Use of mouse genetics for studying inner ear development. *Curr. Top. Dev. Biol.* 57, 45–83.
- Rzadzinska, A.K., Schneider, M.E., Davies, C., Riordan, G.P., Kachar, B., 2004. An actin molecular treadmill and myosins maintain stereocilia functional architecture and self-renewal. *J. Cell Biol.* 164, 887–897.
- Siemens, J., Kazmierczak, P., Reynolds, A., Sticker, M., Littlewood-Evans, A., Muller, U., 2002. The Usher syndrome proteins cadherin 23 and harmonin form a complex by means of PDZ-domain interactions. *Proc. Natl. Acad. Sci. USA* 99, 14946–14951.
- Sjöström, B., Anniko, M., 1990. Morphologically specific vestibular hair cell degeneration in the jerker mouse mutant. *Eur. Arch. Otorhinolaryngol.* 247, 51–55.
- Southard, J.L., 1970. Jackson circler, jc. *Mouse News Lett.* 42, 30.
- Steel, K.P., Kros, C.J., 2001. A genetic approach to understanding auditory function. *Nat. Genet.* 27, 143–149.
- Torres, M., Gomez-Pardo, E., Gruss, P., 1996. *Pax2* contributes to inner ear patterning and optic nerve trajectory. *Development* 122, 3381–3391.
- Tsukamoto, K., Suzuki, H., Harada, D., Namba, A., Abe, S., Usami, S., 2003. Distribution and frequencies of *PDS (SLC26A4)* mutations in Pendred syndrome and nonsyndromic hearing loss associated with enlarged vestibular aqueduct: a unique spectrum of mutations in Japanese. *Eur. J. Hum. Genet.* 11, 916–922.
- Usami, S., Abe, S., Weston, M.D., Shinkawa, H., Van Camp, G., Kimberling, W.J., 1999. Non-syndromic hearing loss associated with enlarged vestibular aqueduct is caused by *PDS* mutations. *Hum. Genet.* 104, 188–192.
- Vazquez, A.E., Luebke, A.E., Martin, G.K., Lonsbury-Martin, B.L., 2001. Temporary and permanent noise-induced changes in distortion product otoacoustic emissions in CBA/CaJ mice. *Hear. Res.* 156, 31–43.
- Wang, J., Mark, S., Zhang, X., Qian, D., Yoo, S.J., Radde-Gallwitz, K., Zhang, Y., Lin, X., Collazo, A., Wynshaw-Boris, A., Chen, P., 2005. Regulation of polarized extension and planar cell polarity in the cochlea by the vertebrate PCP pathway. *Nat. Genet.* 37, 980–985.
- Witmer, P.D., Doheny, K.F., Adams, M.K., Boehm, C.D., Dizon, J.S., Goldstein, J.L., Templeton, T.M., Wheaton, A.M., Dong, P.N., Pugh, E.W., Nussbaum, R.L., Hunter, K., Kelmenson, J.A., Rowe, L.B., Brownstein, M.J., 2003. The development of a highly informative mouse simple sequence length polymorphism (SSLP) marker set and construction of a mouse family tree using parsimony analysis. *Genome Res.* 13, 485–491.
- Xu, P.X., Adams, J., Peters, H., Brown, M.C., Heaney, S., Maas, R., 1999. *Eya1*-deficient mice lack ears and kidneys and show abnormal apoptosis of organ primordia. *Nat. Genet.* 23, 113–117.
- Zheng, Q.Y., Johnson, K.R., Erway, L.C., 1999. Assessment of hearing in 80 inbred strains of mice by ABR threshold analyses. *Hear. Res.* 130, 94–107.
- Zheng, L., Sekerkova, G., Vranich, K., Tilney, L.G., Mugnaini, E., Bartles, J.R., 2000. The deaf jerker mouse has a mutation in the gene encoding the espin actin-bundling proteins of hair cell stereocilia and lacks espins. *Cell* 102, 377–385.
- Zhou, R., Abbas, P.J., Assouline, J.G., 1995a. Electrically evoked auditory brainstem response in peripherally myelin-deficient mice. *Hear. Res.* 88, 98–106.
- Zhou, R., Assouline, J.G., Abbas, P.J., Messing, A., Gantz, B.J., 1995b. Anatomical and physiological measures of auditory system in mice with peripheral myelin deficiency. *Hear. Res.* 88, 87–97.